Sensors and Materials, Vol. 34, No. 7 (2022) 2897–2909
MYU Tokyo

S & M 3013

Liquid Level Intelligent Detection for Oil Tank Based on Empirical Mode Decomposition and Deep Belief Network

Qiwei Zhao*

Ningbo MadeIt Semiconductor Co., Ltd., Ningbo 315000, China

(Received April 1, 2022; accepted May 25, 2022)

Keywords: machine learning algorithm, intelligent detection, ultrasonic Lamb wave, empirical mode decomposition (EMD), deep belief network (DBN)

The liquid level of different types of oil in an oil tank can be judged on the basis of the amplitude of time-domain signals, but the characteristic information obtained by this signal is relatively simple. In addition, the liquid level intelligent detection for oil tanks based on machine learning techniques, such decision tree algorithm, artificial neural network algorithm, and support vector machine, has stimulated considerable research interest. To obtain more characteristic information and improve the liquid level detection rate of different medium signals in an oil tank, a liquid level intelligent detection method based on empirical mode decomposition (EMD) and deep belief network (DBN) for a steel oil tank of 5 mm thickness is provided in this paper. Firstly, the ipsilateral phase detection method of the air-coupled ultrasonic Lamb wave was adopted to detect the oil tank with the help of the A0 model. Then, the intrinsic mode function (IMF) of each order was obtained by analyzing the signals of different media in the oil tank by EMD, and the correlation characteristics of the time/frequency domain signals of each order IMF component were analyzed. Finally, the time/frequency domain signals of the IMF component served as the input signals of the DBN model. The liquid level is divided into 15 sections as the output of DBN. The experimental results of the combination of EMD and DBN show that the liquid levels of different media in the oil tank can be accurately identified and further classified within the range of 10 mm, the detection rate can reach 99%, and the detection range meets the actual testing requirements of the oil tank.

1. Introduction

The rapid development of industrial production has made chemical processes more complex and refined than ever before. The accurate detection of liquid levels can make people more clearly understand the entire production process and progress and formulate production plans, which is conducive to improving production efficiency and ensuring safe production to a certain extent. Therefore, the effective detection of container liquid levels plays a key role in the safety

*Corresponding author: e-mail: zhao.qiwei@icloud.com
https://doi.org/10.18494/SAM3930

ISSN 0914-4935

of industrial production.[1] Under the inevitable trend of industrial production refinement, testing equipment not only needs to have the characteristics of high detection accuracy and noncontact detection but can also adapt to the special environment of high temperature and pressure, dust, and humidity in industrial sites, which poses a great challenge to liquid level detection technology. At present, there are many methods of measuring the liquid level of oil tanks, such differential pressure level detection, ultrasonic level detection, fiber optic level detection, laser level detection, and radar wave level detection.[2,3] The sensing elements used in these methods are usually placed inside the oil tank, and the vessel needs to be retrofitted or redesigned for level inspection, which creates new hidden dangers or increases manufacturing costs. In addition, the sensor inside the vessel is prone to aging, which increases maintenance costs. Therefore, the development of a noncontact level detection technology that does not require container modification is critical for engineering applications.

In noncontact ultrasonic testing, the Lamb wave has been widely used in ultrasonic testing because of its advantages of low loss, high safety, and convenience.[4] At present, the research on the analysis and identification of different medium liquid levels in an oil tank has not achieved satisfactory results. The effectiveness of medium type recognition results in an oil tank is mainly affected by the extraction accuracy of different medium signal features.[5] Although the liquid level of different media in an oil tank can be determined on the basis of the amplitude of the time-domain signal, the characteristic information of the signal is relatively simple. Therefore, it is important to analyze the signal in the frequency domain and obtain more characteristic quantities of different medium signals, which further improve the recognition rate of liquid level.[6] For the extraction of eigenvalues, scholars have conducted extensive research. By analyzing the eigenvalues of A-scan signals and combining them with a vector machine, pipeline defects can be identified effectively, as shown by Dey *et al.*[7] Liang *et al.* analyzed the defect signal amplitude and peak arrival time as feature quantities to identify various types of debonding defects.[8] He *et al.* performed empirical mode decomposition (EMD) on the acquired signal and then extracted the maximum amplitude, center frequency, and signal energy of each intrinsic mode function (IMF) component signal as eigenvalues for defect identification. By performing wavelet packet transformation on the signal, the approximation and detail coefficients are used as the feature quantities of the extracted samples to identify the defects of the composite material, and it is verified that the method can effectively identify different defects.[9]

However, owing to the inherent characteristics of Lamb waves, local time scale-based EMD can generate an appropriate basis function according to this characteristic, which has good adaptability for the analysis of nonlinear and nonstationary signals.[10] Therefore, in this paper, EMD is used to process signals of different media in an oil tank to obtain the IMF of each order. The correlations between the time-domain and frequency-domain signals of IMF components and the original signals are compared and analyzed, and the time-domain and frequency-domain signals are used as the input values of the deep belief network (DBN) for decision-making, to realize the identification and classification of different medium levels in oil tanks.

2. Intelligent Detection of Liquid Level in Oil Tank

2.1 Analysis of ultrasonic Lamb wave detection mechanism

The ultrasonic Lamb wave refers to the elastic wave propagating in the platelike waveguide structure. The propagating waveform is divided into the transverse and longitudinal waves, which are formed by the particle vibration direction perpendicular and parallel to the surface of the plate. As a type of ultrasonic guided wave, the ultrasonic Lamb wave has frequency dispersion and multimodal characteristics.[11] Its group and phase velocities exhibit dissimilarity, and multiple vibrational modes appear simultaneously during propagation. Usually, the propagation of ultrasonic Lamb waves in a columnar pipe structure can be approximated as propagation in a plate. When the propagating medium is vacuum or air, the propagation of ultrasonic Lamb waves can be considered to be a non-attenuation or less attenuation system. However, when the propagation medium is a layered medium or a liquid medium, the ultrasonic Lamb wave will leak into the liquid or other layered medium, which makes the propagation system attenuate greatly. Therefore, the complex frequency or wave number processing can be introduced,[12] which can be calculated as

$$x(t) = \alpha + i \cdot \beta, \tag{1}$$

where α and β are the real and virtual wave numbers, respectively, where β represents the energy attenuation. The virtual wave number β can be set to zero if the system has no attenuation or has a small attenuation. The virtual wave number β is also large when the system has a large attenuation.

In the level detection of an oil tank, the outside of the tank wall is in contact with air, the inside is in contact with a liquid, and ultrasonic Lamb waves propagate in a multilayer medium (air, tank wall, or liquid). There is a large attenuation during the propagation of ultrasonic Lamb waves. Therefore, the energy attenuation degree in the process of Lamb wave propagation can determine whether its propagation path passes through a liquid. Figure 1 shows the propagation diagram of an ultrasonic Lamb wave in an oil tank.

2.2 Empirical mode decomposition preprocessing

Geddes *et al.* proposed the use of EMD, which served as an adaptive signal decomposition method.[13] The signal $x(t)$ is firstly processed by EMD to obtain several IMFs. Theoretically, EMD can achieve arbitrarily high temporal and frequency resolutions and provide a new method of analysis and guidance for nonstationary and nonlinear signals. Each IMF must meet two criteria: (1) the number of zero intersections and limit points is less than or equal to a difference across the entire data segment, and (2) the average of the envelopes consisting of a local minimum and a local maximum at any point is zero.

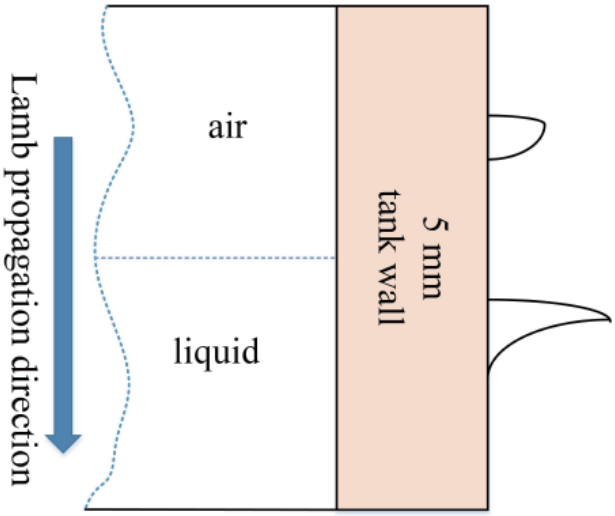

Fig. 1. (Color online) Schematic of Lamb wave propagation in an oil tank.

The steps of EMD are as follows: (1) On the basis of all the maxima and minima of the original signal, fit the maximum and minimum envelopes by a cubic spline function and subtract the mean envelope of the original signal from the mean of the upper and lower envelopes. The network generates the first new low-frequency signal removed as the initial signal. (2) After the condition of the IMF is satisfied, record the condition as a component of the IMF. The IMF is then subtracted from the original signal to obtain the remaining signal as the new signal. (3) Follow the above steps to obtain the following sequence, and repeat the cycle to obtain the original signal components meeting the IMF. After the EMD preprocessing, the original signal $x(t)$ can be expressed as

$$s(t) = \sum_{i=1}^{N} IMF_i(t) + r_N(t). \tag{2}$$

In addition, for ease of understanding, the flowchart of the EMD algorithm is shown in Fig. 2.

2.3 DBN level discriminant model

After the ultrasonic Lamb wave signal propagating in the oil tank is decomposed by EMD, a series of local time-frequency characteristics of the IMF signal can be obtained. By constructing a multifeature fusion evaluation model, the mapping relationship between feature vectors and target detection values can be established. In 2021, Xing *et al.* proposed a typical deep learning network for the intelligent fault diagnosis of machines, i.e., DBN.[14] In compliance with DBN, low-level signals are learned by greedy pretraining layer by layer to form a more abstract high-level representation. The unsupervised self-learning process can avoid the expert experience required for traditional feature fusion and achieve intelligent detection. During the model

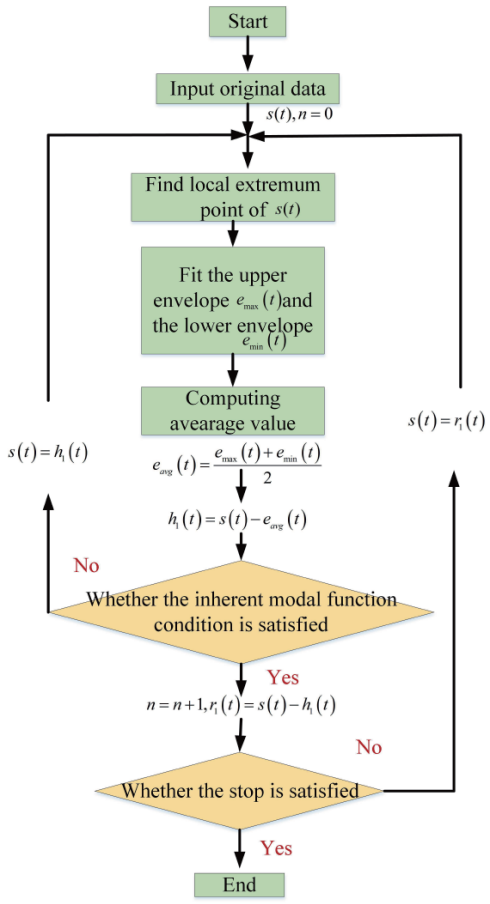

Fig. 2. (Color online) EMD algorithm flowchart.

training, DBN can build a parametric model between the characteristic input of the ultrasonic Lamb wave signal and the oil tank liquid level through multilayer nonlinear mapping.

DBN is composed of a series of restricted Boltzmann machine (RBM) models,[15] which belong to a multilayer perceptron neural network. DBN includes a visible layer (v) and a hidden layer (h). Nodes in different layers are connected by weight, but nodes in the same layer are not connected. The RBM model structure is shown in Fig. 3, and the total numbers of neurons in the visible and hidden layers are N and M, respectively. $v = (v_1,v_2,\ldots,v_i,\ldots,v_N)^T$ represents the state vector of the visual layer, $h = (h_1,h_2,\ldots,h_j,\ldots,h_M)^T$ defines the state vector of the hidden layer, $w = (w_{ij})$, $i \in [1, N]$, and $j \in [1, M]$ represents the weight matrix between the visual and hidden layers, and the bias vectors for the visual and hidden layers are a and b, respectively.

In the training phase, DBN maps the relevant information extracted from the visual layer to the hidden layer, extracts the information again in the hidden layer, maps it to the visual layer, then reconstructs the input data in the visual layer, and constantly repeats the mapping and reconstruction.[16] The DBN model, which consists of three RBMs stacked on top of each other, is shown in Fig. 4.

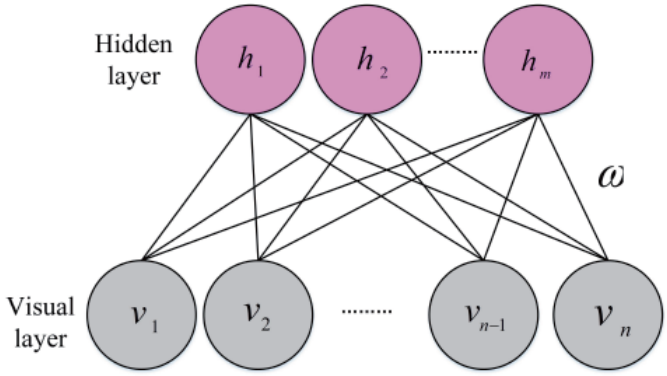

Fig. 3. (Color online) RBM model structure.

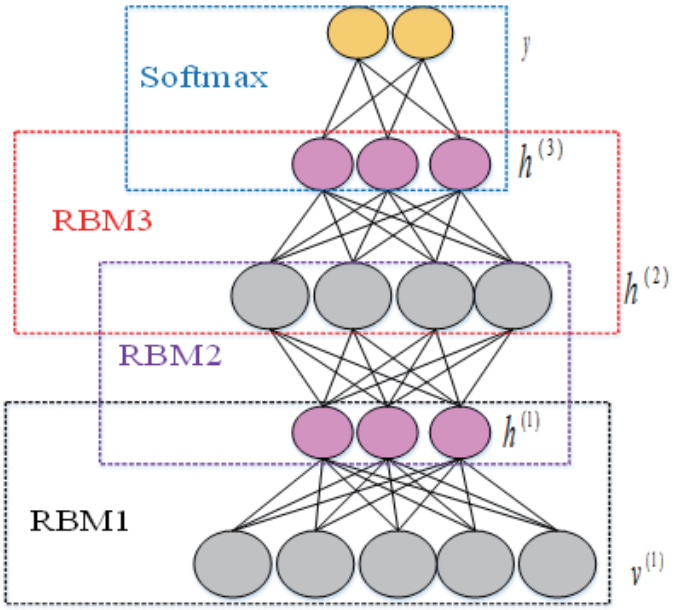

Fig. 4. (Color online) DBN structure.

The visual layer can be used as the feature input layer. The lower RBM learns the IMF time-frequency feature vector after EMD, and its output result is used as the input data of the upper RBM. After multilayer greedy learning, a more intuitive feature representation is formed. The DBN learning process consists of two parts, namely, forward stacking RBM learning and backward fine-tuning learning. The forward stacking process is an unsupervised learning process that requires no involvement of label data. However, the fine-tuning of the parameters of the network model is carried out through the marked data, i.e., the reverse fine-tuning. The learning process of the forward stacking RBM is defined as follows.

(1) Determining the structural parameters of the RBM network, such as feature input sample $s = (x_1, x_2, ..., x_N)^T$, learning rate ε, and the numbers of nodes in the visual and hidden layers (N and M, respectively).

(2) Initializing the network parameters, i.e., visual layer initial state $v^{(1)} = s$, in which the variable superscript represents the number of trainings, random initialization weight w, and bias vectors a, b.
(3) Achieving the probability obtainment of the visual layer elements and hidden layers nodes.

$$\begin{aligned} P\left(h_j^{(1)}=1\middle|v^{(1)}\right)&=\delta\left(b_j+\sum_i v_i^{(1)}\cdot w_{ij}\right)\\ P\left(v_i^{(2)}=1\middle|h^{(1)}\right)&=\delta\left(a_i+\sum_j h_j^{(1)}\cdot w_{ij}\right)\\ P\left(h_j^{(2)}=1\middle|v^{(2)}\right)&=\delta\left(b_j+\sum_i v_i^{(2)}\cdot w_{ij}\right) \end{aligned} \tag{3}$$

(4) Updating the parameters w, a, and b.

$$\begin{aligned} \dot{w}&=w+\varepsilon\left(P\left(h_j^{(1)}=1\middle|v^{(1)}\right)\left(v^{(1)}\right)^T-P\left(h_j^{(2)}=1\middle|v^{(2)}\right)\left(v^{(2)}\right)^T\right)\\ \dot{a}&=a+\varepsilon\left(v^{(1)}-v^{(2)}\right)\\ \dot{b}&=b+\varepsilon\left(P\left(h_j^{(1)}=1\middle|v^{(1)}\right)-P\left(h_j^{(2)}=1\middle|v^{(2)}\right)\right) \end{aligned} \tag{4}$$

(5) Recalculating the activation probability of each layer node and updating the network parameters until the K iteration is completed, which takes $h^{(2)}$ as the input $v^{(1)}$ of the higher RBM, and continuing to train the next RBM. After DBN, the softmax layer is served as a network classifier, which allows the backward fine-tuning of network parameters with labeled data. Suppose that the output vector of the last layer of DBN is defined as

$$h^l(x)=\frac{1}{1+\exp\left(b^l+w^l h^{l-1}(x)\right)}. \tag{5}$$

After the ith sample is learned by the lth layer RBM, the probability that y_i belongs to the category $k\in(1,2,...,c)$ is defined as

$$p\left(y_i=k\middle|h^l(x_i),c^l\right)=\frac{e^{V_k^l\cdot h^l(x_i)+c^l}}{\sum_{k=1}^{c}e^{V_k^l\cdot h^l(x_i)+c^l}}. \tag{6}$$

Here, V is the weight parameter of the softmax layer, which selects the category corresponding to the maximum probability as the output. The cross-entropy function is used to represent the lth

layer error function, and the gradient descent method is used to fine-tune the parameters from 1 to *l*th layers.

3. Level Detection Experimental Platform

In this paper, the air-coupled ultrasonic Lamb wave ipsilateral phasing method is adopted, i.e., the probe arrangement is one-shot and one-off phase placement over the surface of the oil tank, the Lamb wave applies the A0 mode, and the air-coupled ultrasonic transducer with a frequency of 400 kHz is selected.[17] The level detection platform of the oil tank consists of a signal generator, a signal amplifier, an air-coupled high-power ultrasonic transducer (JPR-600C), NAUT21 control software, and a high-performance PC, as shown in Fig. 5. First, the digital drive signal generated by the signal generator is amplified by the amplifier to produce a sufficiently large signal. In addition, the transmit and receive air-coupled ultrasonic transducers are symmetrically mounted on the fixing plate with an inclination of 7.2°, the two-probe center is 12 mm from the tank wall, and the two transducer centers are 135 mm apart. The experimental device is a high-sensitivity noncontact air-coupled detection system provided by Japan Probe Co., Ltd. with a frequency of 400 kHz, an applied voltage of 200 V, and a wafer size of 14 × 20 mm^2. Moreover, it is necessary to set up a 5 mm scale bar on a steel tank, start marking the first scale at 33 mm from the bottom of the tank, and make a scale mark every 10 mm upwards, and after setting the software parameters, follow the steps of the experiment.

4. Results and Discussion

By changing the heights of different media, the water, oil, and air layers in the tank are measured. When the amplitudes of the leakage Lamb waves of three different media are different, the amplitudes of the direct wave signals received by the air-coupled ultrasonic receiving transducer in the same media can be averaged through multiple measurements. The waveforms of three different media are shown in Fig. 6. To facilitate comparison, the amplitudes

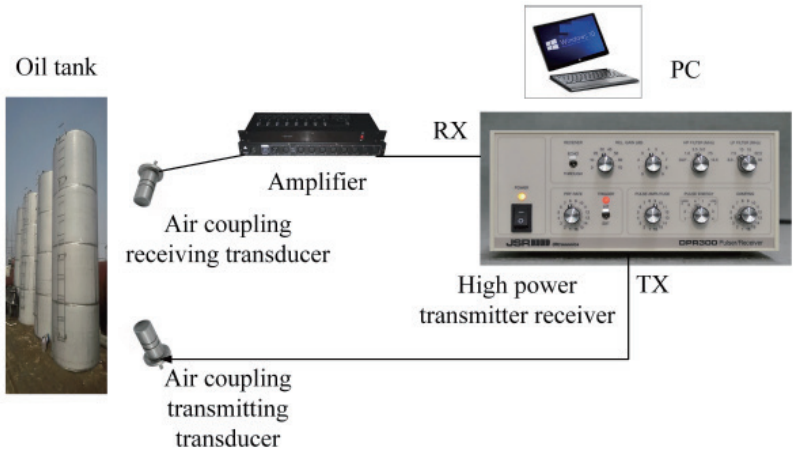

Fig. 5. (Color online) Detection platform.

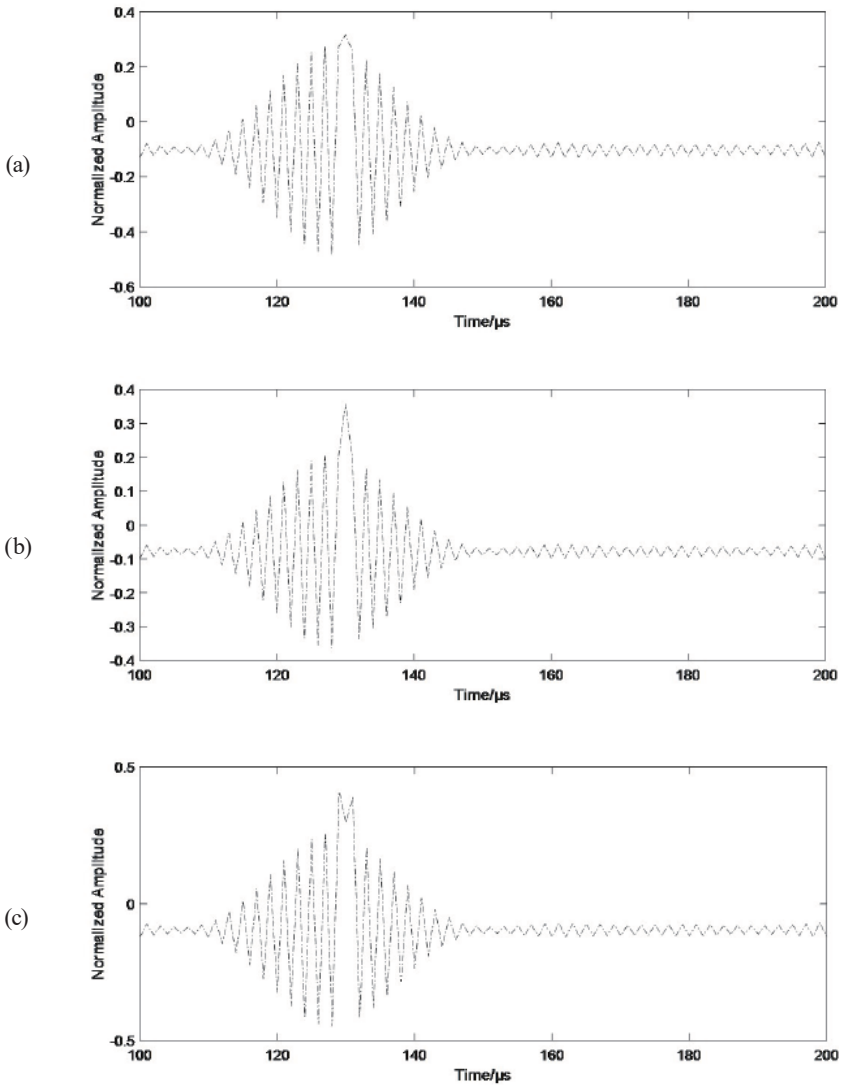

Fig. 6. Ultrasonic echo time-domain signals of different media. (a) Waveform diagram of water medium. (b) Waveform diagram of oil medium. (c) Waveform diagram of air medium.

of the obtained return waves of different media are normalized. Figure 6 shows that the normalized amplitude of the direct wave signal received by the probe is 0.36 when there is air in the tank. When there is oil in the tank, the normalized amplitude of the direct wave signal received by the probe is 0.40. When the tank is filled with water, the normalized amplitude of the direct wave signal received by the probe is 0.30. From the amplitude of each medium signal, the signals of three different media in the tank can be roughly distinguished.

4.1 Identification and classification of different medium signals

To distinguish the echo signals of the three types of media accurately, a total of 24 sample data of eight direct wave signals of water medium, oil medium, and air medium were taken.

Taking the waveform with oil as the acquisition medium in this experiment as an example, EMD was performed on the direct wave signal to obtain the correlation between each order IMF component and the original signal, as shown in Fig. 7. As can be seen from Fig. 7, the correlation between the first four IMF components and the original signal is very high, whereas the correlation between the last four IMF components and the original signal is very low, which can be ignored basically. Therefore, EMD is carried out when the medium of the oil tank is water, and the first four IMF components are analyzed. The first four IMF components of the signal are shown in Fig. 8. Since the information in the frequency domain is more stable and easier to analyze than that in the time domain, the corresponding spectrum diagram of the signal in Fig. 8 is obtained by fast Fourier transform, as shown in Fig. 9.

The time-domain and frequency-domain characteristic information parameters of the IMF component can be represented by the number of zero-crossings, maximum energy, and center frequency. Then, the three feature vectors of the direct wave signal with water medium were calculated as shown in Table 1. According to the characteristic information extraction of ultrasonic direct wave signals in different media of the oil tank, eight groups of samples, water, oil, and air, are selected. Therefore, 24 groups of samples are composed of two parts, i.e., one part is the training sample set composed of 15 groups of data and the other part consists of nine groups of data to form a test sample set. The output of the training sample is shown in Table 2 when the medium of the oil tank is water, oil, or air.

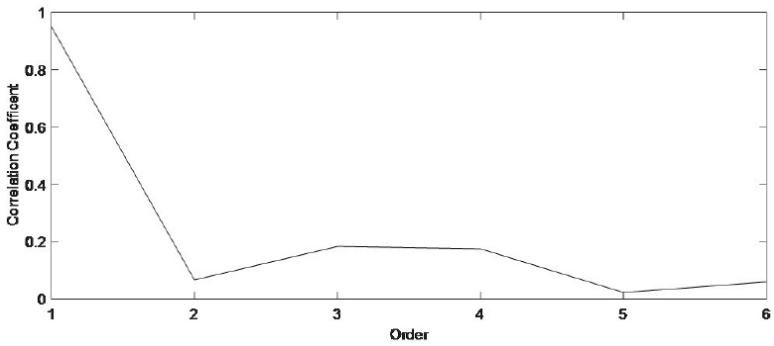

Fig. 7. Correlation diagram between IMF components and the original signal.

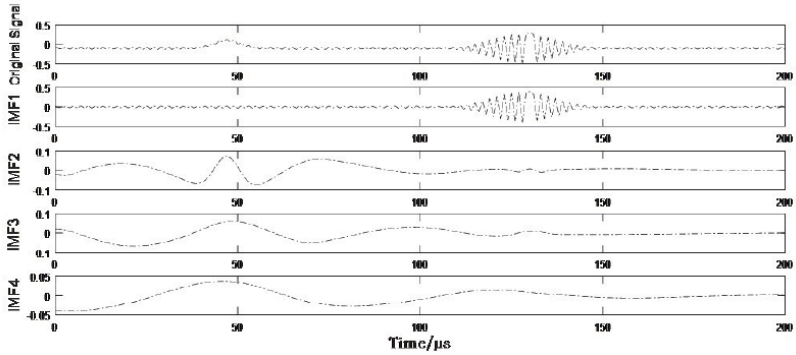

Fig. 8. Ultrasonic echo and EMD decomposition results of water medium.

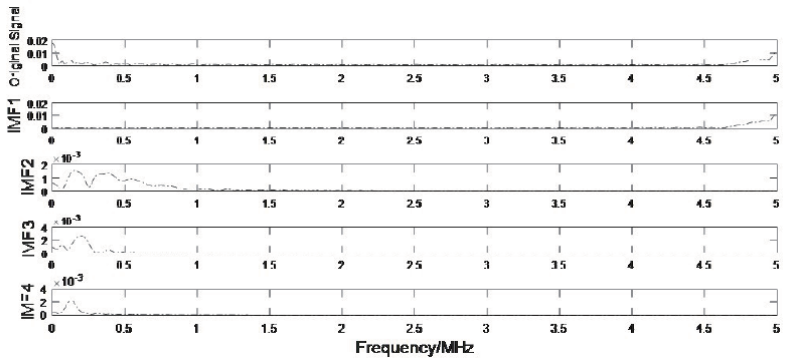

Fig. 9. Spectrum diagram of IMF components decomposed by direct wave EMD in water medium.

Table 1
Characteristic values in time and frequency domains.

Characteristic value	IMF1	IMF2	IMF3	IMF4
Number of zero-crossings	204	128	46	22
Maximum value energy	0.01	0.0015	0.0024	0.0022
Center frequency	4.65	0.35	0.22	0.11

Table 2
Coding results of different media.

Medium type	Water	Oil	Air
Medium coding	100	010	001

4.2 Liquid level detection analysis of DBN

The collected 150 data samples were divided into the training and test sets; the training set samples accounted for 62.5% and the test set samples accounted for 37.5%. The characteristic values extracted after EMD transformation were taken as the network input. The samples were divided into 15 categories according to liquid level height, and the network output was the medium coding of 15 categories. The number of network iterations was set to 5000. The training accuracy, test accuracy, and loss function of network training were varied as shown in Fig. 10, which also shows that as the number of iterations increases, the loss value of the network loss function decreases gradually, and the training accuracy increases gradually. Particularly in the early iteration algorithm, the loss function value drops rapidly, and the training accuracy increases rapidly, which indicates that the extracted eigenvalue and testing level have a better mapping relationship. Finally, the training and test accuracies are higher than 90%. Moreover, the loss function value is still in a state of decline, which continues to reduce the iteration error. The test results after 5000 iterations are shown in Fig. 11(a). Under the current number of iterations, the training accuracy rate is 92.8%. When the liquid level is half full, the misclassification of adjacent categories occurs. However, after 10000 iterations, all categories were correctly identified, as shown in Fig. 11(b).

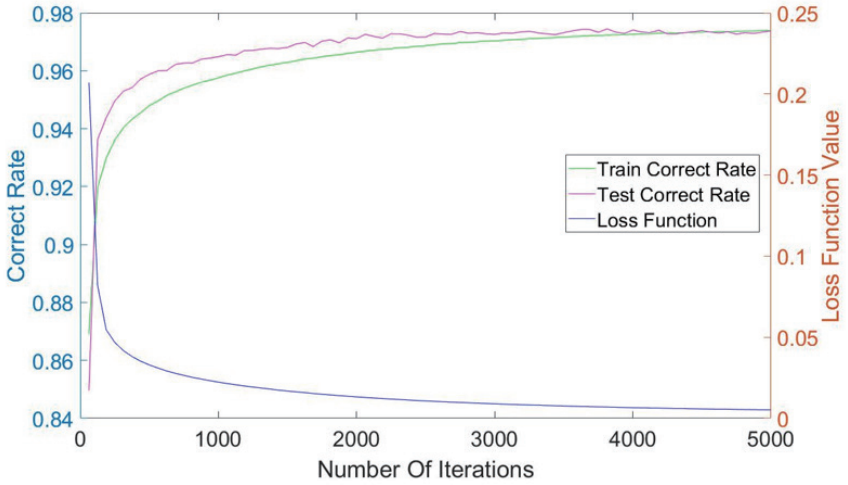

Fig. 10. (Color online) Network training process.

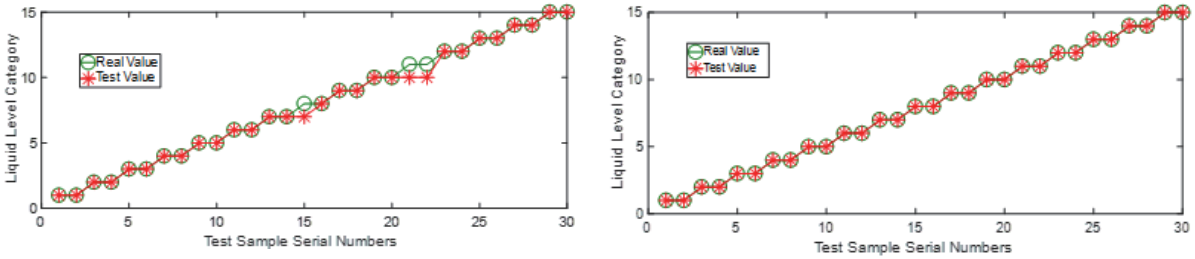

Fig. 11. (Color online) Final test results of (a) 5000 and (b) 10000 iterations.

5. Conclusions

Aiming at the problem of online liquid level detection in an oil tank, an air-coupled ultrasonic Lamb wave intelligent detection method based on EMD and DBN was proposed, which has a good effect on determining the liquid levels of different media in an oil tank. First, the EMD algorithm is used to obtain the signal component of the IMF and to further extract the local time-frequency characteristics of the ultrasonic Lamb signal; then, the extracted feature is served as the input of the DBN. The theoretical and experimental research studies show that when the number of iterations is 5000 times, the proposed method can identify the basic level, and only a handful of states appear incorrectly nearby. However, when the number of iterations is 10000, the accuracy of liquid level height detection reaches 100%. For the accuracy of liquid level detection, we will focus on the regression application of the deep learning network in the future.

Acknowledgments

This work was supported by the Chongqing Natural Science Foundation Project (No. cstc2021jcyj-msxmX0301) and the Science and Technology Research Project of the Chongqing Education Commission (Nos. KJQN202101216 and KJQN202101223).

References

1 M. Wei, Z. Deng, J. Zheng, and W. Zhou: IEEE Trans. Appl. Supercond. **32** (2022) 1. https://doi.org/10.1109/TASC.2021.3131398
2 M. Vogt and M. Gerding: IEEE Microwave Mag. **18** (2017) 38. https://doi.org/10.1109/MMM.2017.2711978
3 H. Yi, L. Xia, J. Xu, C. Yu, Y. Wu, C. Li, and L. Zhu: IEEE Photonics J. **9** (2017) 1. https://doi.org/10.1109/JPHOT.2017.2732681
4 X. Gu and F. Cegla: IEEE Trans. Instrum. Meas. **69** (2020) 6843. https://doi.org/10.1109/TIM.2020.2975389
5 P. Esmaili, F. Cavedo, and M. Norgia: IEEE Trans. Instrum. Meas. **69** (2020) 4379. https://doi.org/10.1109/TIM.2019.2945414
6 P. Chawah, R. Briand, V. Dupé, F. Boudin, M. Cattoen, F. Lizion, and H.-C. Seat: IEEE Sens. J. **21** (2021) 1580. https://doi.org/10.1109/JSEN.2020.3020512
7 S. Dey, S. Santra, P. K. Guha, and S. K. Ray: IEEE Trans. Electron Devices **66** (2019) 3568. https://doi.org/10.1109/TED.2019.2922704
8 F. Liang, P. Zhao, Y. Feng, and W. Wang: IEEE Trans. Ind. Electron. **69** (2022) 8535. https://doi.org/10.1109/TIE.2021.3108700
9 Q. He, H. Meng, Z. Hu, and Z. Xie: IEEE Trans. Instrum. Meas. **68** (2019) 3456. https://doi.org/10.1109/TIM.2018.2879548
10 Z. Tian: IEEE Trans. Intell. Transp. Syst. **22** (2021) 5566. https://doi.org/10.1109/TITS.2020.2987909
11 S. Liao, L. Ou, and L. Xu: IEEE Trans. Instrum. Meas. **70** (2021) 1. https://doi.org/10.1109/TIM.2020.3016153
12 B. D. Majumder and J. K. Roy: IEEE Trans. Instrum. Meas. **70** (2021) 1. https://doi.org/10.1109/TIM.2020.3041107
13 J. Geddes, J. Mehlsen, and M. S. Olufsen: IEEE Trans. Biomed. Eng. **67** (2020) 3016. https://doi.org/10.1109/TBME.2020.2974095
14 S. Xing, Y. Lei, S. Wang, and F. Jia: IEEE Trans. Ind. Electron. **68** (2021) 2617. https://doi.org/10.1109/TIE.2020.2972461
15 Y. Guo and Z. Zhang: IEEE Trans. Instrum. Meas. **70** (2021) 1. https://doi.org/10.1109/TIM.2021.3076569
16 Z. Huang, Z. Zhu, C. H. Yau, and K. C. Tan: IEEE Trans. Neural Networks Learn. Syst. **32** (2021) 2847. https://doi.org/10.1109/TNNLS.2020.3007943
17 A. B. Zoubi and V. J. Mathews: IEEE Trans. Ultrason. Ferroelectr. Freq. Control **68** (2021) 829. https://doi.org/10.1109/TUFFC.2020.3015153

About the Author

Qiwei Zhao received his B.S. degree from Northwestern Polytechnical University (Xi'an China), China, and his M.S. degree from Northeastern University (Boston, USA), China, in 2008 and 2011, respectively. He then joined Ningbo MadeIt Semiconductor Co., Ltd., where he is currently an engineer. His research interests include electricity information engineering, semiconductor design, and manufacturing. (zhao.qiwei@icloud.com)